

Article

Not peer-reviewed version

The GPI-Anchored Aspartyl Proteases Encoded by the *YPS1* and *YPS7* Genes of *Candidozyma auris* and Their Role Under Stress Conditions

[Alvaro Vidal Montiel](#) , [Daniel Clark-Flores](#) , [Eulogio Valentín-Gómez](#) , [Juan Pedro Luna-Arias](#) ,
[Erika Rosales-Cruz](#) , [César Hernández-Rodríguez](#) , [Lourdes Villa-Tanaca](#) ^{*} , [Margarita Juárez-Montiel](#) ^{*}

Posted Date: 24 June 2025

doi: 10.20944/preprints202506.1844.v1

Keywords: *candidozyma auris*; yapsin; aspartyl protease; glycosylphosphatidylinositol GPI; cell wall integrity; stress conditions



Preprints.org is a free multidisciplinary platform providing preprint service that is dedicated to making early versions of research outputs permanently available and citable. Preprints posted at Preprints.org appear in Web of Science, Crossref, Google Scholar, Scilit, Europe PMC.

Copyright: This open access article is published under a Creative Commons CC BY 4.0 license, which permit the free download, distribution, and reuse, provided that the author and preprint are cited in any reuse.

Article

The GPI-Anchored Aspartyl Proteases Encoded by the *YPS1* and *YPS7* Genes of *Candidozyma auris* and Their Role Under Stress Conditions

Alvaro Vidal-Montiel ¹, Daniel Clark-Flores ¹, Eulogio Valentín-Gómez ^{2,3},
Juan Pedro Luna-Arias ⁴, Erika Rosales-Cruz ⁵, César Hernández-Rodríguez ¹,
Lourdes Villa-Tanaca ^{1,*} and Margarita Juárez-Montiel ^{1,*}

¹ Laboratorio de Biología Molecular de Bacterias y Levaduras, Departamento de Microbiología, Escuela Nacional de Ciencias Biológicas, Instituto Politécnico Nacional, Prol. de Carpio y Plan de Ayala. Col. Sto. Tomás, 11340, Mexico City, Mexico.

² Departamento de Microbiología y Ecología, Universidad de Valencia, 46100- Burjassot (Valencia) España.

³ Grupo de Investigación Infección Grave, Instituto de Investigación La Fe, 46026-Valencia, Spain.

⁴ Departamento de Biología Celular, Centro de Investigación y de Estudios Avanzados del Instituto Politécnico Nacional (Cinvestav-IPN), 07360, Ciudad de Mexico, México.

⁵ Laboratorio de Investigación en Hematopatología, Departamento de Morfología, Escuela Nacional de Ciencias Biológicas, Ciudad de Mexico, México.

* Correspondence: mvillat@ipn.mx (L.V.-T.); mjuarezm@ipn.mx (M.J.-M.)

Abstract

Candidozyma auris is a multidrug resistance opportunistic pathogen, distinguished from *Candida* yeasts because of their thermotolerance, osmotolerance, and persistence in biotic and abiotic surfaces, attributes that seem linked to the cell wall composition. Here, seven putative genes encoding yapsins, extracellular aspartyl proteases GPI-anchored to the membrane or cell wall, were identified in the genomes of *C. auris* strains CJ97 and 20-1498, from clades III and IV, respectively. *C. auris* *YPS1* gene is orthologous to the *SAP9* of *C. albicans*. The *YPS7* gene is orthologous to *YPS7* of *C. glabrata* and *S. cerevisiae*, so they could coincide in roles. The *CauYPS1* and *CauYPS7* expression increased under nutrient starvation, 1.5 M NaCl, and at 42°C. In silico analysis suggests the interaction of pepstatin A, an aspartyl protease inhibitor, with the catalytic domain of Yps1 and Yps7. This inhibitor, in concert with caffeine, had a subtle effect on the growth of *C. auris* strains. However, these compounds induce alterations in the appearance of the cell wall. Thereby, yapsins *CauYps1* and *CauYps7* may play a role in the cell wall integrity of *C. auris* in stress conditions, and they could be a therapeutic target for the design of new antifungal or antivirulence agents.

Keywords: *Candidozyma auris*; yapsin; aspartyl protease; glycosylphosphatidylinositol GPI; cell wall integrity; stress conditions

1. Introduction

Aspartyl proteases are enzymes that have gained attention due to their involvement in the infection processes of pathogenic fungi. Yeast aspartyl proteases, or yapsins, are anchored to the cell wall through covalent bonds to β -1,6-glucans or the cell membrane via the GPI (glycosylphosphatidylinositol) group. They participate in cell wall remodeling by processing proteins located here, a process essential for the integrity of this structure during morphogenesis, and adaptation to environmental changes adhesion, biofilm development, and nutrient acquisition by degrading extracellular proteins, such as host tissue and immune defense proteins [1–4]. Since 1990, when Egel-Mitani et al. [5] described in *S. cerevisiae* GPI-aspartyl proteases capable of partially complementing *kex2* mutants by processing the α -mating factor precursor when it is overexpressed,

it has been shown that, in contrast to other aspartyl proteases with affinity to hydrophobic residues, *S. cerevisiae* yapsins's cleave dibasic residues [6]. Then, Bourbonnais et al. [7] showed that Yps1 of *S. cerevisiae* also cleaves monobasic residues, unlike Kex2. Similarly, Sap9 and Sap10 of *C. albicans* partially complemented kex2 mutants by processing monobasic and dibasic residues of peptides. Although Sap9 and Sap10 *C. albicans* still retain the nomenclature of secreted aspartyl protease (Sap), proteases without GPI modification, in silico, molecular and biochemical studies have shown that they differ from other Sap members. For example, they exhibit enzymatic activity over a broad range of pH, even at neutral (physiological) pH, have their distinct cleavage preferences, and are cell surface-associated proteases that function in cell wall integrity and interaction with human epithelial cells and neutrophils [2].

Yapsins are synthesized as zymogens, containing an N-terminal signal peptide removed after translocation into the endoplasmic reticulum by a signal peptidase. These enzymes present a catalytic domain with two aspartic residues, or at least one, in the Asp-Thr(Ser)-Gly(DT(S)G) consensus, which is crucial for their enzymatic function, the N-terminal propeptide removed in the Golgi apparatus at the dibasic or monobasic residues by Kex2 or by yapsin peptidases [1,2,8]. The C-terminal is a hydrophobic domain for transient binding to the ER membrane and the ω site where the protein is linked to the GPI anchor. The ω site is at the consensus sequence [NSGADC]-[GASVIETKDLF]-[GASV]-X(4,19)-[FILMVAGPSTCYWN]. Like other aspartyl proteases from the A1 family, they contain four cysteines forming disulfide bridges [1,9,10]. It has been observed that yapsins, like Saps, of human pathogenic yeasts, occur as multigene families, and the expansion of these families seems to be related to their success as pathogens and in their survival [11].

Candidozyma auris (syn. *Candida auris*) is an opportunistic multidrug-resistant pathogen first described in 2009 by Satoh et al. [12]. Since then, it has been identified as responsible for hospital outbreaks worldwide, causing systemic infections with high mortality. As a result, the World Health Organization issued an epidemiological alert to identify, notify, and timely manage cases and outbreaks caused by *C. auris* [13]. In addition, *C. auris* is thermotolerant and halotolerant, contributing to its ability to colonize various environments. This yeast also forms pseudohyphae and aggregates under specific conditions [14–17]. Among other characteristics that distinguish *C. auris* from other pathogenic yeast are its capacity to form multilayered biofilm, cause invasive infections without forming mycelium, and immune evasion, features attributed in part to the yeast cell wall [18–20]. *C. auris* isolates have been grouped into six main geographical clades through phylogenetic analyses. Strains of each clade differ by hundreds of thousands of single nucleotide polymorphisms (SNPs). Genetic differences between clades have been linked to differences in the cell wall and membrane composition [13,21].

In contrast to *C. albicans*, whose genome carries 10 genes encoding Saps, *C. auris* has a multigene family of 14 or 15 genes encoding these proteins [20,22]. Particularly, Sap3 contributes to extracellular proteolytic activity, biofilm formation, and virulence in animal models, suggesting that its inhibition could be a promising therapeutic strategy [22]. Given the importance of secreted aspartyl proteases as virulence factors in *C. auris*, this study addressed the identification of GPI-anchored aspartyl proteases encoding genes of two strains of the clades III and IV each one and through the use of the aspartyl protease inhibitor, pepstatin A, and the expression analysis of the *C. auris* YPS1 and YPS7 genes, which seem to be the most probable orthologous of YPS1, YPS7 and SAP9 of *S. cerevisiae* and other *Candida*, which encode the standout GPI-proteases in cell wall homeostasis [23,24].

Understanding the molecular mechanisms by which YPS1 and YPS7 contribute to stress tolerance in *Candida auris* could help to develop therapeutic and control strategies against this yeast.

2. Materials and Methods

2.1. Strains

In this work were used the *C. auris* CJ97 [25,26] and 20-1498 [27] strains isolated from the blood of hospitalized patients from Spain and Mexico, grouped into Clades III and IV, respectively. They

were stored frozen at -70°C and routinely grown in YPD (yeast extract 1%, peptone 2%, dextrose 2%) at 37°C with shaking at 100 rpm.

2.2. In Silico Analysis

The sequences of putative yapsin-coding genes and putative targets of yapsins were identified through BLAST analysis and hidden Markov models (HMMs) in the previously reported genomes of the two *C. auris* strains CJ97 and 20-1498 (GCA_034640365.1) [28], and *C. auris* B11220 strain from clade II (GCA_003013715.2). Sequences of the *Saccharomyces cerevisiae* yapsin genes (ScYPS 1, 2, 3, 6 and 7) from the genome (<https://www.yeastgenome.org/>) were used as a template. The predicted open reading frame and 1000 bp upstream (considered the promoter sequence) of each selected gene were analyzed using various tools. The SignalP v6.0 (February 10, 2024; <https://services.healthtech.dtu.dk/services/SignalP-6.0/>) [29], ScanProsite (February 13, 2024; <https://prosite.expasy.org/scanprosite/>), and NetGPI v1.1 (March 15, 2024; <https://services.healthtech.dtu.dk/services/NetGPI-1.1/>) [30] were used to found motives in protein sequences, while, to explain a possible differential expression of the genes, promoters were analyzed in the YEASTRACT server looking for probable transcription factors binding sites (TFBSs) (June 27, 2024; <https://saves.mbi.ucla.edu/>) [31]. Moreover, the percentage of similarity and identity of protein sequences was stated with MatGat v2.01 [32].

2.3. Phylogeny of *C. auris* Putative Yapsins

First, proteins were aligned with Clustal X [33]. The most conserved regions of GPI-anchored aspartyl peptidases of *S. cerevisiae*, *C. glabrata* (*Nakaseomyces glabratus*), *C. albicans*, and *C. auris* CJ97 were used to construct the phylogeny, with the IQ-TREE software [34], using the best substitution model (WAG+F+R4). One thousand bootstrap replicates were applied, and the tree was visualized with Figtree v1.4.5. Accession numbers of protein sequence used, *S. cerevisiae*: ScYps1 (NP_013221.1), ScYps2 (NP_010428.3), ScYps3 (NP_013222.1), ScYps6 (NP_012305.3), ScYps7 (NP_010636.1); *C. albicans*: CaSap9 (KAL1572689.1), CaSap10 (XP_717243.1); *C. glabrata* CgYps1 (XP_449529.1), CgYps2 (XP_445750.2), CgYps3 (XP_445764.1), CgYps4 (XP_445765.1), CgYps5 (XP_445766.1), CgYps6 (XP_445767.1), CgYps7 (XP_444870.1), CgYps8 (XP_445768.1), CgYps9 (XP_445769.1), CgYps10 (XP_445770.1), CgYps11 (XP_445771.1); and *C. auris* B11220: CauYps1 (XP_028889414.2), CauYps2 (XP_028891323.2), CauYps3 (XP_028888407.2), CauYps4 (XP_028892789.1), CauYps5 (XP_028891322.2), CauYps6 (XP_028890862.2) CauYps7 (XP_028892266.2).

2.4. Prediction of the Secondary and Tertiary Structure of Putative Yapsins

The mature forms of putative yapsins CauYps1 (amino acids 52-108 and 199-566) and CauYps7 (amino acids 57-527) were used to predict the secondary and tertiary structure of *C. auris* Yps proteins. Prediction of the secondary and tertiary structure was carried out in ENDscript v3.0 (July 18, 2024; <https://endscript.ibcp.fr/ESPrpt/ENDscript/>) [35] and the SWISS-MODEL servers, respectively (Oct 12, 2024; <https://swissmodel.expasy.org/>) [36], using the better models selected by the programs, as templates. Once the theoretical tertiary structures were obtained, their quality was analyzed using the SAVES server (15 October 2024; <https://saves.mbi.ucla.edu/>).

2.5. Molecular Docking of *C. auris* Putative Yps1 and Yps7

The 3D models of predicted mature and CauYps7 from *C. auris*, obtained from the SWISS-MODEL server, were used for molecular docking analysis with the specific and reversible inhibitor of aspartic proteases, pepstatin A, retrieved from the PDB (PRD_000557). This was modified using the Avogadro software to prepare it for interaction [37]. The docking process was performed in ChimeraX [38] with the aid of AutoDock Vina [39].

To test the potential activity of yapsins on a probable molecular target, a molecular docking analysis was conducted using a peptide

(MALWMRLLPLLALLLWGPDPAAAFVNQHLCGSHLVEALYLVCGERGFFYTPKTRREAEDLQVGQVELGGGPGAGSLQPLALEGSLQKRGIVEQCCTSICSLYQLENYCN) of the proinsulin hormone (AAW83741.1). The docking was then performed using the H-Dock server (28 October 2024; <http://hdock.phys.hust.edu.cn/>) [40], which predicts possible molecular interactions between two proteins.

2.6. Evaluation of *C. auris* Growth Under Different Conditions

The *C. auris* strains CJ97 and 20-1498 were pre-cultured for 24 h in YPD medium at 37°C with shaking at 100 rpm. A 96-well plate was inoculated with 100 µl of yeast at 0.05 of OD₆₀₀ containing YPD medium with different compounds at a final concentration as indicated: 1.5 M NaCl, 12 mM caffeine, 10 mM H₂O₂, 0.05% SDS all from Sigma-Aldrich (St. Louis, MO, USA), in the presence and absence of 25 µM pepstatin A (ChemCruz, Dallas, Tx, USA). YPD without any compounds was considered the growth control, and YPD without compounds and inoculum was used as the sterility control. Plates were incubated 20 h, at 37°C, with shaking, in a Multiskan FC 5111900 (Thermo Fisher Scientific Waltham, MA, USA) and OD₆₂₀ measured. Three independent replicates were performed, and the standard deviation and significance were determined by two-way ANOVA with SigmaPlot software.

2.7. Expression of *YPS1* and *YPS7* Genes by RT-qPCR

Starting from a 48 hours pre-culture in a YPD medium, an early stationary phase culture in YPD was obtained by inoculating yeast at an OD₆₀₀ of 0.05 after 15 h of incubation at 37°C and 100 rpm. These non-proliferating cultures were harvested at 2400 g for 5 min, washed twice, and inoculated into an equal volume of YNB (USBiological, Swampscott, MA, USA) with 2% dextrose (Sigma-Aldrich, St. Louis, MO, USA) as a carbon source and 0.5% (NH₄)₂SO₄ (Gibco, Waltham, MA, USA) or BSA (Sigma-Aldrich, St. Louis, MO, USA) as a nitrogen source (YNB+C+N), YNB with only carbon (YNB+C-N) or nitrogen (YNB-C+N), and neither carbon nor nitrogen (YNB-C-N), also were tested. The cultures were incubated at 37°C with shaking at 100 rpm. To evaluate the effect on gene expression at 42°C and NaCl, cells were transferred to YPD without/with 1.5 M NaCl, incubated at 37°C, or to YPD alone and incubated at 42°C. Two independent experiments in triplicate were performed for each condition.

Cells were harvested after 3 and 6 h to extract total RNA using the Schmitt et al. method [41], based on hot phenol extraction. Cells from the desired condition were resuspended in AE buffer (50 mM sodium acetate, 10 mM EDTA) and disrupted with 10% SDS and pH 5 phenol. Samples were placed in a water bath at 65°C for 5 min and immediately ultra-frozen for 10 min. After centrifugation at 12,879 g for 10 min, the aqueous phase was recovered, followed by two washes with chloroform-isoamyl alcohol. Then, absolute and 70% ethanol with DEPC-treated water were added to precipitate and wash RNA. Finally, it was resuspended in nuclease-free water, and its quantity and quality were assessed.

All the RT-qPCR reagents were from Thermo Fisher Scientific (Waltham, MA; USA) SYBR Select Master Mix. cDNA synthesis was done using 2 µg of DNA-free RNA, treated with DNaseI, the RevertAid reverse transcriptase, and the oligo (dT)18 primer, according to the manufacturer's instructions. SYBR Select Master was used according to the supplier's instructions, using the primers *YPS1* Fw: CTCGAACGAGGAGGACATCG, Rev: TGCTTACAGTCACCGAG; and *YPS7* Fw: CCTTAAAACTTCAGAGCAGTAGG, Rev GACCACACCAACAAACGCTC. The reaction was subjected to initial denaturation of 95°C for 5 min, with subsequent Forty-five cycles at 95°C for 30, annealing at 59°C for 30 s, and extension at 72°C for 1 min 15 s, in a thermal cycler Corbett Research RG-6000 (Corbett Robotic Inc, San Francisco, CA, USA). The data were analyzed with the 2-ΔΔCt methodology [42]. The *ACT1* gene (CJ196_0003605) [43] was used as the normalizing gene, and the control conditions were YNB+C+N at 37°C and YPD at 37°C. Reactions were performed in triplicate in two biological experiments.

2.8. Effect of Pepstatin A on the Microscopic Morphology of *C. auris*

Scanning electron microscopy (SEM). Yeast cells were inoculated at 0.05 OD₆₀₀ in YPD medium without or with different concentrations of pepstatin A (12.5, 25, and 50 μ M), 12 mM caffeine, or 0.01% methanol, from an inoculum of 24 h in YPD. Cells were treated for 22 h, harvested, and washed with Sørensen's PBS, then fixed overnight at room temperature by adding 2.5% glutaraldehyde. Cells were washed three times with Sørensen's PBS and sequentially dehydrated with increasing ethanol concentrations, from 50% to 100%. Then, samples were dried for 3 h at 35°C/1350 psi with a critical point dryer K850 (Quorum Technologies, Lewes, UK) and observed using a scanning electron microscope Quanta FEG 250 (FEI Company, Netherlands).

In Atomic force microscopy (AFM). Cells treated or not with 50 mM of pepstatin were harvested and washed three times with sterile distilled water. Cells resuspended in an equal volume of water as a medium were placed on a slide, air drying, and fixed for 1 h with formaldehyde vapors. After, slides were observed (TT-AFM., Workshop, USA).

3. Results

3.1. *C. auris* Presents a Family of YPS Multigene Encoding Putative Yapsins

Genes encoding putative GPI-anchored aspartyl proteases (yapsins) were identified by Blast and HMMs in the genome of three strains of *C. auris*: B11220 (reference genome), CJ97, and 20-1498 from clades II, III, and IV, respectively. We found 15 putative genes encoding aspartyl proteases based on information retrieved from the bioinformatic tools. Seven of these sequences presented the omega site of GPI anchorage (ω). Both CauYps2 and CauYps5 amino acid sequences do not show the typical catalytic aspartic residue of this type of proteases (Figure S1). The putative yapsins ranged in size from 372 to 703 amino acids. *C. auris* yapsins from the three clades showed identities greater than 95.6% and virtually identical motifs, except for CauYps5. CauYps5 from B11220 (clade II) was shorter at the N-terminus than the yapsins from strains CJ97 and 20-1498, and they shared identities of approximately 50% and 60%, respectively (Figure S1).

Additionally, to the two catalytic aspartic residues and the ω site, the N-terminal signal peptide and the typical KR sites, cleavage by Kex2 or autoprocessing at the N-terminal propeptide and the C-terminal, before the ω site, N-glycosylation sites, and low *pI*, all characteristics of the yapsins, were also predicted. The sequences of the *C. auris* CJ97 yapsins were usually more conserved with their cognate sequences in B11220 (Figure S1 and S2); thereby, sequences of the putative yapsins of the last two strains were used for the in silico analysis.

3.2. *Yps1* and *Yps7* of *C. auris* Are Orthologous to the Yapsins of *C. albicans*, *C. glabrata* (*Nakaesomyces glabratus*), and *S. cerevisiae*

To examine the phylogenetic relationship between the putative yapsins of *C. auris* and those of other yeast species, an alignment of the most conserved regions of 25 sequences was performed. This analysis showed that *C. auris* Yps1 is related to *C. albicans* Sap9 and Sap10 (Figure 1A). CauYps1 showed a probable internal loop that could be removed similarly to ScYps1 by cleavage of the monobasic or dibasic residues into its region (Figure 1B and Figure S2). On the other hand, *C. auris* Yps7 is associated with the clade of *C. glabrata* and *S. cerevisiae* Yps7. However, *C. glabrata* and *S. cerevisiae* did not show well-conserved aspartic and disulfide bridges (Figure 1D). Besides, *C. auris* Yps3, Yps4, and Yps6 were less related to yapsin proteins, while *C. auris* Yps2 and Yps5 showed no relation to the yapsins included in the analysis (Figure 1A). The *CauYPS1-CauYPS7* genes are distributed across different chromosomes in the *C. auris* genome (Figure 1C). Although *CauYPS2* and *CauYPS5* are on the same chromosome, there is no phylogenetic relationship between them (Figure 1 and Figure S1).

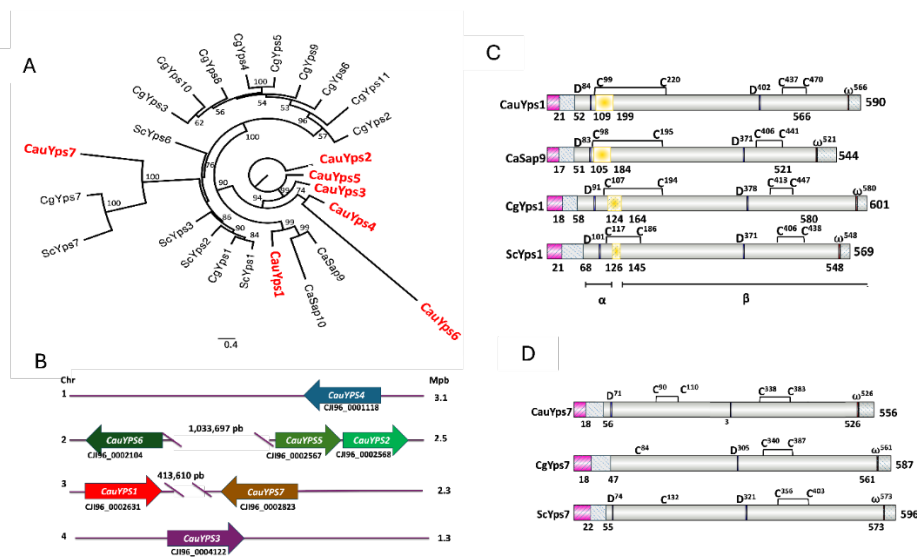


Figure 1. Characteristics of *C. auris* predicted yapsins. **A)** Phylogenetic analysis of the yapsins multigene family of yeasts. The maximum likelihood reconstruction was performed using amino acid sequences of *S. cerevisiae* (Sc), *C. albicans* (Ca), *C. glabrata* (Cg), and *C. auris* (Cau) in the IQ-TREE software with 1000 bootstrap replicates. Figtree services were used for visualization and edition, and bootstrap support >50% was included in branches. Protein accession numbers were indicated in the material and methods section. The scale bar shows the number of substitutions per position. **B)** Schematic representation of *C. auris* YPS gene loci. **C)** Schematic representation of the domains or motifs of predicted CauYps1 and its homologous of *C. albicans* (Sap9), *C. glabrata* (CgYps1) and *S. cerevisiae* (ScYps1). This yapsin undergoes self-processing in an internal loop (yellow rectangle) and remains split into two subunits (α and β) through a disulfide bridge. The numbers below indicate the numbers where processing takes place. Active aspartic residues (D), omega site (ω), and cysteines of the disulfide bridges (C) are indicated: pink rectangle: signal peptide, grey-blue rectangle: propeptide. **D)** Motifs of CauYps7 predicted and its homologous yapsin of *C. glabrata* (CgYps7) and *S. cerevisiae* (ScYps7). CgYps7 and ScYps7 did not show one of the cysteines (C) involved in the disulfide bridges, and CgYPS7 did not show the first catalytic aspartic residue (D).

3.3. The *C. auris* proteins Yps1 and Yps7 Present a Secondary and Tertiary Structure of Aspartyl Proteases, Capable of Binding to the Specific Inhibitor Pepstatin A and Interacting with Other Proteins

The secondary and tertiary structures of mature CauYps1 and CauYps7 were predicted, as mentioned in the methods section. The most conserved regions of the yapsins showed a secondary structure concerning the templates *C. tropicalis* Sap and *C. albicans* Sap5 (Figure S3). In the case of the 3D structure, the templates selected were the *C. tropicalis* Sap and *C. albicans* Sap1, which showed an identity and similarity of 33.5% and 52.7% with Yps1, and 18.2 % and 33.1% with Yps7, respectively. The quality of the predicted tertiary structures of CauYps1 and CauYps7, suggested that they are suitable models. The percentage of residues in most favored regions in the Ramachandran plot, the overall quality factor (from ERRAT) and the percentage of residues showing averaged 3D/1D score \geq 0.1 (from VERIFY3D) correspond to 81.9%, 77.86 and 90.07% for CauYps1 and 88.7%, 81.68 and 50.85% for CauYps7.

Both protein structures of CauYps1 and CauYps7, exhibited a bilobed arrangement, forming a catalytic pocket. Each lobe contains one of the two catalytic aspartic residues, both oriented toward the pocket. The molecular docking showed that pepstatin A (hexapeptide inhibitor of aspartyl protease) fits into the pocket of the predicted structures. The binding energy of pepstatin A for Yps1 was -6.5 kJ/mol, while for Yps7, it was -6.9 kJ/mol. Furthermore, the catalytic aspartic residues bind to the statine amino acid of pepstatin A and some amino acids of the proinsulin peptide (Figure 2).

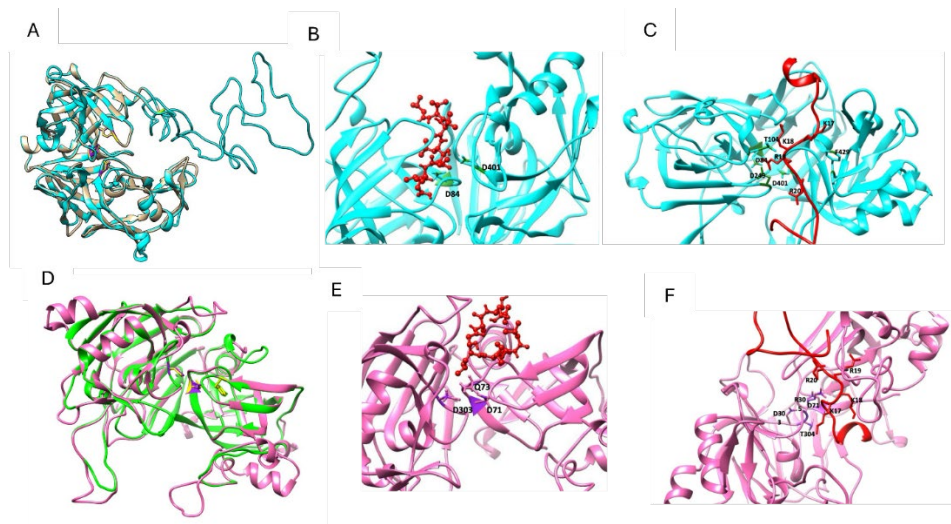


Figure 2. The predicted tertiary structure of the *C. auris* Yps1 and Yps7 and their interaction with the inhibitor pepstatin A and a synthetic substrate. **A)** and **D)** Overlap of the mature CauYps1 (cyan) and the *C. tropicalis* Sap (1J71) (brown) with a rmsd of 0.46 Å°, and CauYps7 (pink) and the *C. albicans* Sap1 (2QZW) with a RMSD of 0.206 Å°. Molecular Docking of the CauYps1 **B)** and CauYps7 **E)** with pepstatin A (red), and **C)** and **F)** with a derived peptide of proinsulin (red), respectively. The catalytic residues Asp84 and 401 of CauYps1 interact with statines 4 and 6 of the inhibitor and with Arg56 of the substrate. In contrast, the catalytic residue Asp303 of CauYps7 interacts with the statine 4 of the inhibitor and Arg46, Ala81, Glu83, and Ser85 of the substrate. Amino acid numbers are given based on the complete protein or peptide sequences.

To infer the possible role of the CauYps1 of *C. auris* and taking in mind the presence of the KR sites in the CauYps1, which could be cleavage by Kex2 or autocatalytically, and also the probable processing of the proinsulin peptide by Yps1 and Yps7 of *C. auris* in the basic or dibasic sites, genes encoding proteins previously described as targets of the *S. cerevisiae* Yps1 and *C. albicans* Sap9 were searched in the *C. auris* genome (Figure 3). After a comparison of these proteins, it was detected the well-known dibasic residues in the α -mating factor of the mentioned yeast, *C. auris* (Figure 3A). Furthermore, the putative cell wall protein Pir and the transmembrane osmosensor Msb2 of *C. auris* could be processed by Yps1 in the earlier protein at the propeptide KR-processing site and at the cleavage domain (CD) in the latter protein, as occurs in *S. cerevisiae* (Figure 3B and C). In contrast, Yps1 could also process the GPI-anchored CauUtr2 and the CauGas1, homologous to the *S. cerevisiae* Utr2 and Gas1, GPI proteins processed by the ScYps1. However, CauGas1 showed a less conserved cleavage site compared to the well-known K353 of ScGas1, but for ScGas1, a second processing site has been proposed, and it is likely that the Gas1 of *C. auris* present it (Figure 3). Protein sequences of *C. glabrata* were included. They showed probable CgYps1 processing sites, thereby being also likely targets of at least this yapsin.

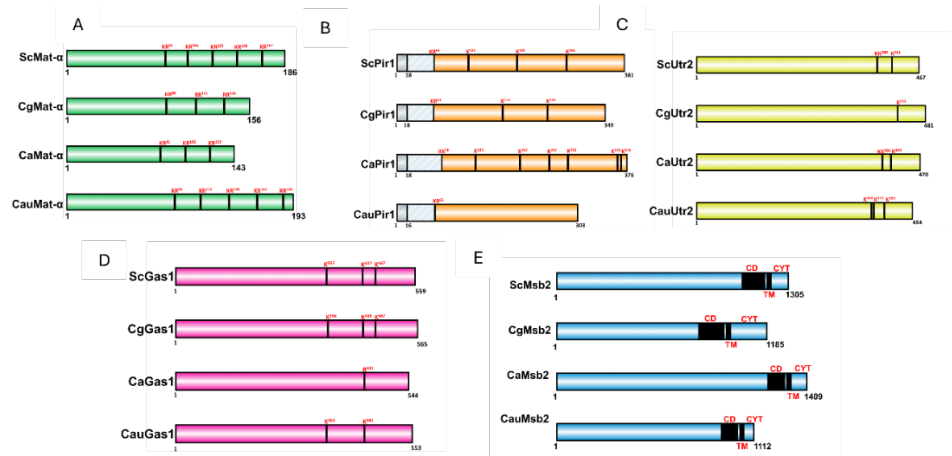


Figure 3. Predicted protein targets of Yps1 of *C. auris*. **A)** The α -mating factor (Mat α) showed dibasic cleavage sites of Kex2 serin carboxypeptidase. ScMat α (AGW24899.1), CgMat α (XP_446929.1), CaMat α (KAL1575323.1), Cau Mat α (QRG37869.1; clade V). **B)** In contrast to other yeasts, the cell wall protein Pir1 of *C. auris* showed only one cleavage site by Yps1, probably involved in processing the prosegment: grey light rectangle. ScPir1 (ONH77051.1), CgPir1 (XP_447520), CaPir1 (XP_712603), CauPir1 (XP_054558182). **C)** The GPI-anchored chitin transglycosidase Utr2 (Crh2) carries two cleavage sites, recognized by Yps1 and Yps2, involved in its secretion. ScUtr2 (AJV34305.1), CgUtr2 (XP_445272.1), CaUtr2 (XP_721748.1), CauUtr2 (XP_028889825). **D)** The GPI-anchored Beta-1,3-glucanotransferase Gas1 of *C. auris* shows probable monobasic recognition sites by Yps1, but they are not conserved with that of the ScGas1. ScGas1 (AJS80525.1), CgGas1 (XP_449946.1), CaGas1 (XP_719043.1), CauGas1 (XP_028892777). **E)** The transmembrane osmosensor Msb2 contains probable dibasic residues in the CD: cleavage domain. After Yps1 processing, the extracellular inhibitor domain is released. ScMsb2 (NP_011528), CgMsb2 (XP_446100), CaMsb2 (XP_722538), CauMsb2 (XP_028892564). Sc: *S. cerevisiae*, Cg: *C. glabrata*, Ca: *C. albicans*, Cau: *C. auris*. IBS v2 was used to draw images.

3.4. Growth of *C. auris* CJ97 and 20-1498 in the Presence of Different Stressor Compounds

C. auris strains were cultured for 20 h at 37°C in the presence of H₂O₂, caffeine, NaCl, and SDS without or with pepstatin A to determine whether aspartyl protease inhibition affected yeast growth. The results showed that H₂O₂, NaCl, and SDS inhibit the growth of *C. auris*. When pepstatin A was also present in media containing H₂O₂ and caffeine, it exhibited a subtle but sustained effect on the growth of the yeasts compared to the controls (without pepstatin A (Figure 4). In contrast, *C. auris* strains grown in media with pepstatin plus SDS and NaCl did not show changes in growth compared to the controls (Figure S3).

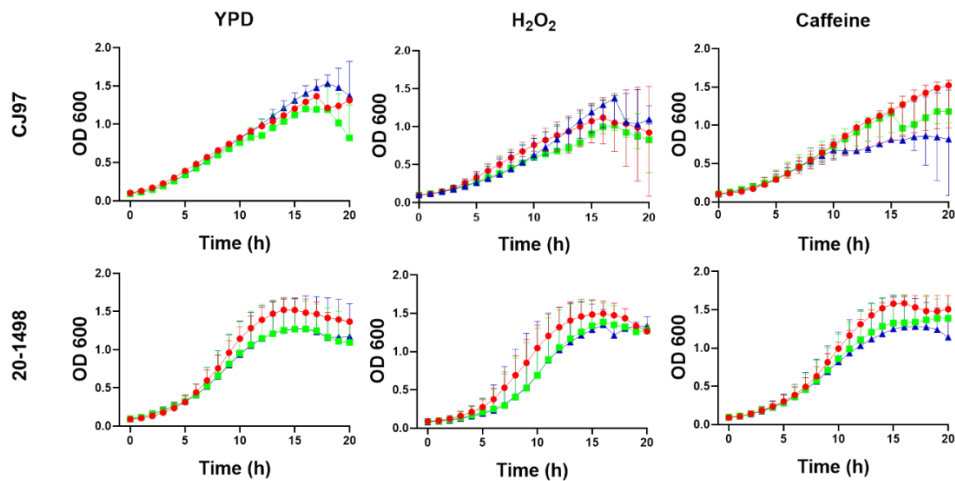


Figure 4. Effect of pepstatin A on the growth of *C. auris* CJ97 (clade III) and 20-1498 (clade IV). Yeasts were grown in YPD medium or YPD supplemented with 10 mM H₂O₂ or 12 mM caffeine, without (red) or with (blue) 25 μM pepstatin A. Green: control with 0.01% methanol, used as the vehicle of pepstatin. The assay was performed in triplicate. Bars indicate standard deviation.

3.5. Differential Expression of YPS1 and YPS7 Genes Under Different Stress Conditions

Yeasts of *C. auris* from clades III and IV were grown in YPD to the early stationary phase and then subjected to different nutritional conditions, 1.5 mM NaCl and at 42°C. Gene expression was conducted 3 and 6 h after stimuli. The results were grouped in a heatmap according to the expression levels of genes (Figure 5). It was observed that the two genes of the CJ97 and 20-1498 strains were differentially expressed. *CauYPS1* of both strains was overexpressed mainly after 6 h without a carbon source compared to the complete medium. *CauYPS7* of 20-1498 (clade IV) showed higher expression than the *CauYPS7* of the CJ97 strain (clade III) after 3 and 6 h of carbon and/or nitrogen starvation. Instead of ammonium sulfate as a nitrogen source, BSA induced the *CauYPS7* of 20-1498 after 3 h, while after 6 h, *CauYPS1* and *CauYPS7* of both strains were repressed.

In general, the *CauYPS1* and *YPS7* genes of both strains were overexpressed after 6 h at 42°C and with NaCl compared to YPD at 37°C, and the expression of *CauYPS7* of the 20-1498 strain was usually higher than that of CJ97. On the other hand, *CauYPS1* and *YPS7* showed repression after treatment of yeasts of the CJ97 and 20-1498 during 3 h with NaCl (Figure 5A and 5B).

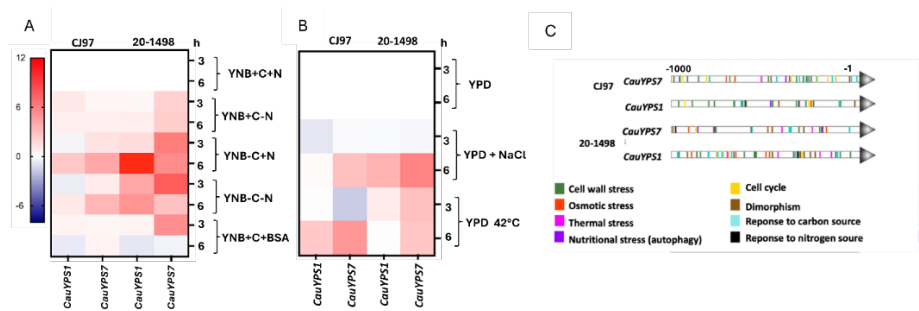


Figure 5. Differential expression of *CauYPS1* and *CauYPS7* genes of the strains CJ97 (clade III) and 20-1498 (clade IV). Heatmap representing the log₂ of the gene expression change determined by RT-qPCR. **A)** RNA extracted from yeast after 3 and 6 h of treatment in YNB medium supplemented with +C= 2% dextrose (as carbon source), +N = 0.5% ammonium sulfate or +BSA= 0.5% BSA (as nitrogen source). Negative signal indicates the absence of the corresponding stimulus. **B)** RNA extracted from yeast after 3 and 6 h of treatment at 37°C in YPD medium without or with 1.5 M NaCl (-NaCl, +NaCl, respectively) or YPD at 42°C. Two independent experiments were carried out in triplicate. **C)** Predicted TFBSs into the 1000 base pairs upstream of the *CauYPS1* and *CauYPS7* genes using the YEASTRACT database.

Expression levels of *C. auris* *YPS1* and *YPS7* genes agreed with their theoretical TFBSs found 1000 bp upstream of the encoding regions. These sites could bind transcription factors linked to, e.g., the response to the cell wall, osmotic and thermal stress, and nutritional stress. Moreover, the *CauYPS1* and *CauYPS7* showed differences in the disposition of the TFBSs along the analyzed upstream regions between the strains (Figure 5C).

3.6. Effect of Pepstatin A on the Microscopic Morphology of *C. auris* 20-1498

C. auris cells were cultured in YPD medium with 12.5, 25, and 50 μM of pepstatin A, and microscopic morphology was observed using scanning electron microscopy (SEM). Cells without the inhibitor plus 0.01% methanol or not were used as a control. In the control conditions, oval-shaped yeasts of approximately 2-2.5 × 3-4 μm were observed with some budding and smooth surfaces. At 12.5 μM, yeasts with a rough appearance were observed at a percentage of 3.5%. This effect was dose-

dependent, as yeasts with this morphology increased to 4.5% at 25 μ M and 6.5% at 50 μ M of pepstatin A. At the highest concentration, concave-looking cells were also observed in 60%.

A synergistic effect was observed when cells were grown in YPD with 25 μ M pepstatin A and 12 mM caffeine. Nearly 90% of the cells showed evident damage to the cell wall, with a wrinkled appearance and presumptive holes, in contrast to the yeast of the medium with only caffeine or pepstatin (Figure 6A).

The effect of pepstatin A on the cell surface topography of *C. auris* was also evaluated by atomic force microscopy (AFM). The roughness of cells with pepstatin A 50 μ M increased in contrast to cell growth in control conditions (Figure 6B). AFM analysis suggests a possible decrease in the size of *C. auris* yeasts when treated with pepstatin A. The length of the yeast would be affected, but not the height. The length varies from 4.2-4.7 μ m of yeast in the control condition to 3.7-3.9 μ m of yeast treated with pepstatin (Figure 6B).

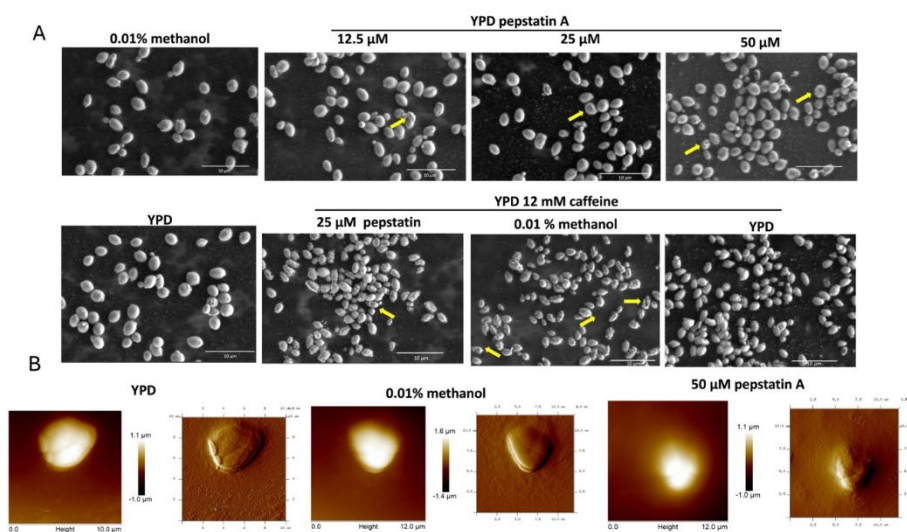


Figure 6. Effect of pepstatin A on the microscopic morphology of *C. auris* 20-1498. **A)** SEM micrographs showing cells with rough and concave surfaces (arrows) after being grown for 22 h in YPD supplemented with pepstatin A and/or caffeine at the indicated concentration. YPD and YPD with methanol are the control conditions. Images of the fixed cells were acquired using an SEM microscopy Quanta FEG 250 (FEI Company, Netherlands). **B)** Height (left) and amplitude (right) images showing the yeast surface of cells grown as before mentioned and treated for AFM observations as indicated in materials and methods. Images were acquired with an atomic force microscope.

4. Discussion

C. auris has emerged as a multidrug-resistant pathogen associated with intra-hospital outbreaks that cause systemic infections with high mortality, becoming a serious public health problem worldwide. This yeast is distinguished from other human pathogenic species by its thermo and osmotolerance, characteristics linked to its ability to survive and persist in various harsh natural and healthcare facilities environments, as well as on the human skin. Combined with the effects of climate change and possibly the excessive use of antifungals, these traits could have contributed to the recent and simultaneous emergence of this yeast as a pathogen in several regions of the world [15–17].

Among other characteristics that distinguish *C. auris* from other pathogenic yeast are its capacity to form multilayered biofilm, to cause invasive infections without forming mycelium, and immune evasion, features contributing to virulence and attributed in part to the yeast cell wall [19]. The use of this structure as a helpful target to control fungal infections has been widely discussed, and because of their contribution to cell wall integrity, GPI-anchored cell wall proteins have been studied for this purpose. The APX001A is a novel agent that inhibits fungal Gwt1 protein, an enzyme

involved in the synthesis of glycosylphosphatidylinositol moiety of GPI-anchored proteins, and treatment of *C. auris* with this compound impairs maturation and localization of GPI proteins, compromising the cell viability [19,44].

Fungal yapsins are extracellular aspartyl proteases GPI-anchored to the yeast cell wall or membrane. These enzymes play nutrient acquisition, dimorphism, and cell wall integrity functions, accounting for virulence in pathogenic fungi [23,45]. Here, we identified seven genes encoding putative yapsins in the genome of *C. auris* B11220 (clade II), which were distributed in four chromosomes. In contrast to the multigene family of *C. glabrata* yapsin, genes of *C. auris* did not show tandem arrangement, suggesting recent duplication [3]. Proteins encoded by these sequences range in size from 372 to 696 amino acids, suggesting potential functional variability among the yapsins of *C. auris*, typical of this multigene family [3,23]. The seven yapsin-encoding sequences were also identified in the genomes of the CJ97 (clade III) and 20-1498 (clade IV) *C. auris* strains, which were practically identical between strains, except for putative CauYps5, it is shorter in B11220 than in CJ97 and 20-1498 (from 697 in the afore strain to 703 amino acids in the two latter). Most of these amino acid sequences exhibited typical characteristics of yapsin-type aspartyl proteases [9,46]: the two conserved aspartic residues within the catalytic domain, except for Yps2 and Yps5, the cysteines responsible for disulfide bridge formation, the signal peptide, propeptides with dibasic or basic processing sites of Kex2 or autoprocessing sites [2,5,46,47], and the omega site characteristic of GPI-anchored proteins. The predicted CauYps2 and CauYps5 do not present the aspartic catalytic residues in the consensus sequence, in contrast to yapsins of *S. cerevisiae* and *C. glabrata*, whose exception is the CgYps7 [3,48]. In addition, the phylogenetic analysis showed that CauYps2 and CauYps5 are not related to the canonical yapsins of the aforementioned yeast, in contrast to the other putative yapsins of *C. auris*. Particularly, putative CauYps1 clustered with the Sap9 and Sap10 of *C. albicans* and the CauYps7 to *S. cerevisiae* and *C. glabrata* Yps7 proteins. It suggests that *YPS1* and *YPS7* of *C. auris* are homologous to *YPS1*, *SAP9*, and *YPS7* of *S. cerevisiae* and *C. albicans*, in agreement with the previously described by Alvarado et al. [20].

In addition, CauYps1 and CauYps7 also showed similar domains to those described for Yps1, Sap9, and Yps7 of other yeasts. Notably, *C. auris* Yps1 showed an internal loop like the Sap9 and Yps1, of *C. albicans* and *S. cerevisiae*, proteins where this region is autoprocessed, generating two subunits linked through a disulfide bridge [2]. Dibasic sites upstream of the ω site seem to contribute to the shedding activity of Yps1 of *S. cerevisiae*, acting on itself and under other proteins [2,49]. For example, Gas1, Utr2, and Msb2, which are a GPI glucan transferase, a GPI chitin transglycosidase, and an osmosensor that regulates the MAPK pathways, respectively, all of which participate in the response of the yeast to different stress conditions [43,50,51]. Furthermore, proteins as the α -mating factor (Mata), a natural target of Kex2, are processed by *S. cerevisiae* Yps1 in deleted mutants of Kex2 [5]. Additionally, the soluble cell wall protein Pir1 of *Saccharomyces* and *C. albicans* is cleaved by Yps1 and Sap9 and Sap10, respectively [4,43]. Similarly, the α -mating factor of *C. auris* and Pir1 could be processed by at least CauYps1, since these proteins showed similar dibasic or monobasic residues recognized by this protease and by Kex2, as has been previously suggested [52].

Additionally, the secondary and tertiary structure of predicted mature forms of Yps1 and Yps7 of *C. auris* showed a similar structure to related Saps of other yeasts of the CUG clade. However, identity percentages are moderate; they are considered adequate for generating predictive models in structural biology, especially for medically relevant proteins such as aspartic proteases [53]. The predicted proteins showed the characteristics of the aspartic proteases of the A1 family, where a catalytic pocket is formed by two non-identical lobes, each one containing one of the two catalytic aspartic residues, and the flap, a loop part of the S1 subsite [10].

The Yps1 and Yps7 tertiary structures interact with pepstatin A and a proinsulin-delivered peptide through their aspartic catalytic residues, in the latter case, by interaction with mono or dibasic residues. The above observations suggest that *C. auris* yapsins are potential targets of this inhibitor peptide, such as the yapsin of *S. cerevisiae*, *Aspergillus oryzae*, and *C. albicans*, besides the affinity of these yapsins for substrates rich in basic residues [4,48,54].

The effect of pepstatin A on the growth and the superficial structures of *C. auris* of the clades III and IV was evaluated to provide insights into the role of yapsins. Pepstatin A is a known inhibitor of aspartic proteases and has helped investigate fungal protease function in superficial structures [55,56]. In the study conditions, the growth of *C. auris* in media containing pepstatin A was not affected, despite other aspartic proteases could be inhibited by pepstatin, such as the previously described SAPs or the vacuolar PrA [22,56]. Furthermore, pepstatin was tested in concert with H₂O₂, caffeine, NaCl, or SDS, conditions where yapsins of other yeast seem to be involved in part through the cell wall integrity [3,23]. Although all the compounds inhibited the growth of both clade III and IV *C. auris* strains, in a similar behavior as observed before [57], together with pepstatin, only peroxide and caffeine influenced the growth of the yeast, suggesting that aspartic proteases may be involved in *C. auris*'s handling stress associated to cell wall. Thus, *C. auris* 20-1498 of the clade IV was subjected to SEM and AFM; while the first has been widely used to observe the superficial structures of yeast, the latter has been used more recently for this purpose with other yeasts, showing been useful [58]. Under control conditions, yeast cells exhibited a typical oval morphology with budding evidence. However, as the concentration of the inhibitor increased, progressive changes in cell morphology were observed, from rough appearance to cells with a concave shape at higher concentrations, increasing when caffeine was added. All of this supports the idea that cell wall integrity depends partially on the activity of aspartic proteases, as has been shown in *P. brasiliensis* and *C. glabrata*. In the latter, using a strain carrying an inactive Yps1^{D91A}, it was evidenced that active yapsins are required for cell wall homeostasis [47,55]. Albeit now, it is not possible to assign this result to a specific aspartyl protease, similar behavior on the cell wall was observed in *C. glabrata* by SEM, as a consequence of the deletion of their 11 yapsin [59] and at least the Sap9 of *C. auris*, here called CauYps1, seem to be involved in the cell wall functionality through its regulation by the HOG pathway [60].

The expression analysis of the genes *YPS1* and *YPS7* of *C. auris* was tested in stress conditions, all known to alter the cell wall remodeling mechanism [61]. The analysis showed that, while the lack of carbon sources induces expression of *YPS1* of both strains CJ97 (clade III) and 20-1498 (Clade IV), the lack of nitrogen source or the presence of BSA induced mainly the *YPS7* of 20-1498 strain. These results agree with the previous reports of expression regulation of genes encoding yapsins 1 and 7 of *C. glabrata* due to dextrose and nitrogen depletion [24,62]. Moreover, *Saccharomyces cerevisiae* *YPS7* is induced by alternate carbon sources such as mucin, a polysaccharide encountered in the host cell [63]. Osmotic stress conditions (NaCl) and thermal stress (42°C) also regulate the expression of *CauYPS1* and *CauYPS7* as before observed in *C. glabrata*; authors suggested that different clinical strains showed differential expression of *CgYPS1* and *CgYPS7* maybe be a consequence in differences in promoter gene sequences [62]. The prediction of TFBSs 1000 bp upstream of the coding sequences of *YPS1* and *YPS7* genes of both strains displayed dissimilar arrangements. However, these promoters may be regulated by the CWI, HOG, and calcineurin pathways implicated in membrane and cell wall stability [61]. The relatively mild change of expression, mainly of *CauYPS1* under these conditions, could be a result of the suggested efficient homeostatic mechanisms that allow *C. auris* to maintain its physiology without the need for a massive transcriptional response, which may be related to post-translational regulation or epigenetic mechanisms [64].

Thus, the *C. auris* genome holds five genes encoding well-conserved putative extracellular yapsins that may be anchored to the membrane or cell wall. Two are less related to aspartyl proteases. Still, some aspartic proteases with an alanine residue instead of the catalytic aspartic have been described [10]. Using pepstatin A, an inhibitor of aspartyl proteases, the growth of both strains of *C. auris* was slightly and differentially affected, mainly in the presence of H₂O₂ and caffeine, and the cell wall became rough with depressions; these results suggest a role of aspartic proteases in maintaining cell wall integrity. Other well-known conditions to induce the reorganization of the *Candida* spp. cell walls are nutrient, temperature, and osmotic stress [61], conditions that differentially regulate the *CauYPS1* and *CauYPS7* expression between the tested strains. These findings showed specific clade transcriptome response; the strain 20-1498 (IV) usually overexpressed the gene *YPS7* in more

conditions than the strain CJ97 (III). Jenull et al. (2021) suggest that the transcriptional profile, even in a limited set of genes, to different types of stress could be necessary for the pathogenesis, antifungal response, and survival of *C. auris* of each clade in adverse environments [64]. Although a direct relation between yapsins and the cell wall of *C. auris* might require mutants of the encoding genes, we showed that *C. auris* yapsins, as other aspartic proteases, could interact with pepstatin A. Treating *C. auris* strains of clades III and IV with this inhibitor in conditions that induce cell wall remodeling, such as caffeine, affects cell growth and wall integrity. Furthermore, other conditions affecting the cell wall, such as starvation, high temperature, and osmotic stress, induced the expression of yapsins genes *YPS1* and *YPS7* of *C. auris*. Identifying GPI-anchored aspartic proteases as a viable target for inhibition suggests a potential strategy for treating *C. auris* infections since the cell wall is key for thermal and osmotolerance and its persistence in skin and clinical environments.

In conclusion, yapsins CauYps1 and CauYps7 may play a role in the cell wall integrity of *C. auris* in stress conditions, and they could be a therapeutic target for the design of new antifungal or antivirulence agents.

Supplementary Materials: The following supporting information can be downloaded at the website of this paper posted on Preprints.org. Figure S1: Characteristics of predicted yapsins of three *C. auris* strains of clades II, III and IV; Figure S2: Predicted secondary structure and motifs of yeast yapsins; Figure S3: Effect of pepstatin A on the growth of *C. auris* in the presence of different compounds.

Author Contributions: conceptualization, L.V.-T., M.J.-M. and C.H.-R.; writing—original draft preparation, A.V.-M., L.V.-T. and M.J.-M.; writing—review and editing, A.V.-M., D.C.-F., L.V.-T., M.J.-M., C.H.-R., J.P.L.-A. and E.V.-G.; bioinformatic analysis, A.V.-M. and D.C.-F.; Effect of pepstatin and cell wall stressor on the growth an microscopic morphology, A.V.-M.; total RNA extraction and relative expression analysis, A.V.-M, E.R.-F.; project administration, L.V.-T., M.J.-M. and C.H.-R.; funding acquisition, L.V.-T. and M.J.-M. All authors have read and agreed to the published version of the manuscript.

Funding: This work was supported by SIP20251179, SIP20251308, SIP20240946, and SIP20242205 (Instituto Politécnico Nacional, Mexico), CBF-2025-I-2871, Bordallo-Landa-Guillén Foundation (grant 2025-07).

Data Availability Statement: We encourage all authors of articles published in MDPI journals to share their research data. In this section, please provide details regarding where data supporting reported results can be found, including links to publicly archived datasets analyzed or generated during the study. Where no new data were created, or where data is unavailable due to privacy or ethical restrictions, a statement is still required. Suggested Data Availability Statements are available in section “MDPI Research Data Policies” at <https://www.mdpi.com/ethics>.

Acknowledgments: I Dr. Mayahuel Ortega Avilés and Dr. Juan Vicente Méndez Méndez for their help in processing the samples for SEM and AFM and for image acquisition, at the Centro de Nanociencias y Micro y Nanotecnologías, IPN, Mexico.

Conflicts of Interest: The authors declare no conflicts of interest.

References

1. Hube, B.; Naglik, J. *Candida albicans* proteinases: Resolving the mystery of a gene family. **2001**. Microbiology, 147, 1997–2005. <https://doi.org/10.1099/00221287-147-8-1997>
2. Albrecht, A.; Felk, A.; Pichova, I.; Naglik, J. R.; Schaller, M.; de Groot, P.; MacCallum, D.; Odds, F. C.; Schäfer, W.; Michel, M.; Hube, B. Glycosylphosphatidylinositol-anchored proteases of *Candida albicans* target proteins necessary for both cellular processes and host-pathogen interactions. **2006**. *J Biol Chem*, 281, 688–694. <https://doi.org/10.1074/jbc.M509297200>
3. Kaur, R.; Ma, B.; Cormack, B. P. A family of glycosylphosphatidylinositol-linked aspartyl proteases is required for virulence of *Candida glabrata*. **2007**. *Proc Natl Acad Sci U S A*, 104, 7628–7633. <https://doi.org/10.1073/pnas.0611195104>

4. Schild, L.; Heyken, A.; de Groot, P. W.; Hiller, E.; Mock, M.; de Koster, C.; Horn, U.; Rupp, S.; Hube, B. Proteolytic cleavage of covalently linked cell wall proteins by *Candida albicans* Sap9 and Sap10. **2011**. *Eukaryot Cell*, 10, 98–109. <https://doi.org/10.1128/ec.00210-10>
5. Egel-Mitani, M.; Flygnering, H. P.; Hansen, M. T. A novel aspartyl protease allowing KEX2-independent MF alpha propheromone processing in yeast. **1990**. *Yeast*, 6, 127–137. <https://doi.org/10.1002/yea.320060206>
6. Olsen, V.; Loh, Y. P. In vivo processing of nonanchored Yapsin 1 (Yap3p). **2000**. *Arch Biochem Biophys*, 375, 315–321. <https://doi.org/10.1006/abbi.1999.1665>
7. Bourbonnais, Y.; Ash, J.; Daigle, M.; Thomas, D. Y. Isolation and characterization of *S. cerevisiae* mutants defective in somatostatin expression: cloning and functional role of a yeast gene encoding an aspartyl protease in precursor processing at monobasic cleavage sites. **1993**. *EMBO J*, 12(1), 285–294. <https://doi.org/10.1002/j.1460-2075.1993.tb05655.x>
8. Gagnon-Arsenault, I.; Tremblay, J.; Bourbonnais, Y. Fungal yapsins and cell wall: A unique family of aspartic peptidases for a distinctive cellular function. **2006**. *FEMS Yeast Res*, 6, 966–978. <https://doi.org/10.1111/j.1567-1364.2006.00129.x>
9. de Groot, P. W. J.; Brandt, B. W. ProFASTA: A pipeline web server for fungal protein scanning with integration of cell surface prediction software. **2012**. *Fungal Genet Biol*, 49, 173–179. <https://doi.org/10.1016/j.fgb.2011.12.009>
10. Rawlings, N. D.; Salvesen, G. Handbook of proteolytic enzymes. **2013**. Academic Press.
11. Parra-Ortega, B.; Cruz-Torres, H.; Villa-Tanaca, L.; Hernandez-Rodriguez, C. Phylogeny and evolution of the aspartyl protease family from clinically relevant *Candida* species. **2009**. *Mem Inst Oswaldo Cruz*, 104, 505–512 <https://doi.org/10.1590/S0074-02762009000300018>
12. Satoh, K.; Makimura, K.; Hasumi, Y.; Nishiyama, Y.; Uchida, K.; Yamaguchi, H. *Candida auris* sp. nov., a novel ascomycetous yeast isolated from the external ear canal of an inpatient in a Japanese hospital. **2009**. *Microbiol Immunol*, 53, 41–44. <https://doi.org/10.1111/j.1348-0421.2008.00083.x>
13. Santana, D. J.; Zhao, G.; O'Meara, T. R. The many faces of *Candida auris*: Phenotypic and strain variation in an emerging pathogen. **2024**. *PLoS Pathog*, 20, e1012011. <https://doi.org/10.1371/journal.ppat.1012011>
14. Yue, H.; Bing, J.; Zheng, Q.; Zhang, Y.; Hu, T.; Du, H.; Wang, H.; Huang, G. Filamentation in *Candida auris*, an emerging fungal pathogen of humans: Passage through the mammalian body induces a heritable phenotypic switch. **2018**. *Emerg Microbes Infect*, 7, 1–13. <https://doi.org/10.1038/s41426-018-0187-x>
15. Casadevall, A.; Kontoyiannis, D. P.; Robert, V. On the emergence of *Candida auris*: Climate change, azoles, swamps, and birds. **2019**. *mBio*, 10. <https://doi.org/10.1128/mbio.01397-19>
16. Arora, P.; Singh, P.; Wang, Y.; Yadav, A.; Pawar, K.; Singh, A.; et al. Environmental isolation of *Candida auris* from the coastal wetlands of Andaman Islands, India. **2021**. *mBio*, 12. <https://doi.org/10.1128/mBio.03181-20>
17. Lockhart, S. R.; Chowdhary, A.; Gold, J. A. The rapid emergence of antifungal-resistant human-pathogenic fungi. **2023**. *Nat Rev Microbiol*, 21, 818–832. <https://doi.org/10.1038/s41579-023-00960-9>
18. Horton, M. V.; Johnson, C. J.; Zarnowski, R.; Andes, B. D.; Schoen, T. J.; Kernien, J. F.; et al. *Candida auris* cell wall mannosylation contributes to neutrophil evasion through pathways divergent from *Candida albicans* and *Candida glabrata*. **2021**. *mSphere*, 6, e0040621. <https://doi.org/10.1128/mSphere.00406-21>
19. Dakalbab, S.; Hamdy, R.; Holigová, P.; Abuzaid, E. J.; Abu-Qiyas, A.; Lashine, Y.; Mohammad, M. G.; Soliman, S. S. Uniqueness of *Candida auris* cell wall in morphogenesis, virulence, resistance, and immune evasion. **2024**. *Microbiol Res*, 127797. <https://doi.org/10.1016/j.micres.2024.127797>
20. Alvarado, M.; Gómez-Navajas, J. A.; Blázquez-Muñoz, M. T.; Gómez-Molero, E.; Fernández-Sánchez, S.; Eraso, E.; Munro, C. A.; Valentín, E.; Mateo, E.; de Groot, P. W. J. The good, the bad, and the hazardous: comparative genomic analysis unveils cell wall features in the pathogen *Candidozyma auris* typical for both baker's yeast and *Candida*. **2024**. *FEMS Yeast Res*, 24, foae039. <https://doi.org/10.1093/femsyr/foae039>
21. Pezzotti, G.; Kobara, M.; Nakaya, T.; Imamura, H.; Fujii, T.; Miyamoto, N.; Adachi, T.; Yamamoto, T.; Kanamura, N.; Ohgitani, E.; Zhu, W.; Kawai, T.; Mazda, O.; Nakata, T.; Makimura, K. Raman metabolomics of *Candida auris* clades: Profiling and barcode identification. **2022**. *Int J Mol Sci*, 23, 11736. <https://doi.org/10.3390/ijms231911736>

22. Kim, J. S.; Lee, K. T.; Bahn, Y. S. Secreted aspartyl protease 3 regulated by the Ras/cAMP/PKA pathway promotes the virulence of *Candida auris*. **2023**. *Front Cell Infect Microbiol*, 13, 1257897. <https://doi.org/10.3389/fcimb.2023.1257897>
23. Krysan, D. J.; Ting, E. L.; Abeijon, C.; Kroos, L.; Fuller, R. S. Yapsins are a family of aspartyl proteases required for cell wall integrity in *Saccharomyces cerevisiae*. **2005**. *Eukaryot Cell*, 4, 1364–1374. <https://doi.org/10.1128/EC.4.8.1364-1374.2005>
24. Askari, F.; Rasheed, M.; Kaur, R. The yapsin family of aspartyl proteases regulate glucose homeostasis in *Candida glabrata*. **2022**. *J Biol Chem*, 298, 101593. <https://doi.org/10.1016/j.jbc.2022.101593>
25. Ruiz Gaitán, A. C.; Moret, A.; López Hontangas, J. L.; Molina, J. M.; Aleixandre López, A. I.; Cabezas, A. H.; et al. Nosocomial fungemia by *Candida auris*: First four reported cases in continental Europe. **2017**. *Rev Iberoam Micol*, 34, 23–27. <https://doi.org/10.1016/j.riam.2016.11.002>
26. Caballero, U.; Eraso, E.; Quindós, G.; Jauregizar, N. In vitro interaction and killing-kinetics of amphotericin B combined with anidulafungin or caspofungin against *Candida auris*. **2021**. *Pharmaceutics*, 13, 1333. <https://doi.org/10.3390/pharmaceutics13091333>
27. Ayala-Gaytán, J. J.; Montoya, A. M.; Martínez-Resendez, M. F.; Guajardo-Lara, C. E.; Treviño-Rangel, R. de J.; Salazar-Cavazos, L.; et al. First case of *Candida auris* isolated from the bloodstream of a Mexican patient with serious gastrointestinal complications from severe endometriosis. **2021**. *Infection*, 49, 523–525. <https://doi.org/10.1007/s15010-020-01525-1>
28. Casimiro-Ramos, A.; Bautista-Crescencio, C.; Vidal-Montiel, A.; González, G. M.; Hernández-García, J. A.; Hernández-Rodríguez, C.; Villa-Tanaca, L. Comparative genomics of the first resistant *Candida auris* strain isolated in Mexico: Phylogenomic and pan-genomic analysis and mutations associated with antifungal resistance. **2024**. *J Fungi*, 10, 392. <https://doi.org/10.3390/jof10060392>
29. Teufel, F.; Almagro Armenteros, J. J.; Johansen, A. R.; Gíslason, M. H.; Pihl, S. I.; Tsigirig, K. D.; Winther, O.; Brunak, S.; von Heijne, G.; Nielsen, H. SignalP 6.0 predicts all five types of signal peptides using protein language models. **2022**. *Nat Biotechnol*, 40(7), 1023–1025. <https://doi.org/10.1038/s41587-021-01156-3>
30. Gíslason, M. H.; Nielsen, H.; Almagro-Armenteros, J. J.; Johansen, A. Prediction of GPI-Anchored proteins with pointer neural networks. **2021**. *Curr Res Biotechnol*, 3, 10.1016/j.crbiot.2021.01.001.c
31. Monteiro, P. T.; Oliveira, J.; Pais, P.; Antunes, M.; Palma, M.; Cavalheiro, M.; Teixeira, M. C. YEASTRACT+: A portal for cross-species comparative genomics of transcription regulation in yeasts. **2020**. *Nucleic Acids Res*, 48, D642–D649. <https://doi.org/10.1093/nar/gkz859>
32. Campanella, J. J.; Bitincka, L.; Smalley, J. MatGAT: An application that generates similarity/identity matrices using protein or DNA sequences. **2003**. *BMC Bioinformatics*, 4, 1–4. <https://doi.org/10.1186/1471-2105-4-29>
33. Larkin, M. A.; Blackshields, G.; Brown, N. P.; Chenna, R.; McGettigan, P. A.; McWilliam, H.; Valentin, F.; Wallace, I. M.; Wilm, A.; Lopez, R.; Thompson, J. D.; Gibson, T. J.; Higgins, D. G. Clustal W and Clustal X version 2.0. **2007**. *Bioinformatics*, 23, 2947–2948. <https://doi.org/10.1093/bioinformatics/btm404>
34. Nguyen, L. T.; Schmidt, H. A.; von Haeseler, A.; Minh, B. Q. IQ-TREE: A fast and effective stochastic algorithm for estimating maximum-likelihood phylogenies. **2015**. *Mol Biol Evol*, 32, 268–274. <https://doi.org/10.1093/molbev/msu300>
35. Robert, X.; Gouet, P. Deciphering key features in protein structures with the new ENDscript server. **2014**. *Nucleic Acids Res*, 42, W320–W324. <https://doi.org/10.1093/nar/gku316>
36. Waterhouse, A.; Bertoni, M.; Bienert, S.; Studer, G.; Tauriello, G.; Gumienny, R.; Heer, F. T.; de Beer, T. A. P.; Rempfer, C.; Bordoli, L.; Lepore, R.; Schwede, T. SWISS-MODEL: homology modelling of protein structures and complexes. **2018**. *Nucleic Acids Res*, 46, W296–W303. <https://doi.org/10.1093/nar/gky427>
37. Hanwell, M. D.; Curtis, D. E.; Lonie, D. C.; Vandermeersch, T.; Zurek, E.; Hutchison, G. R. Avogadro: an advanced semantic chemical editor, visualization, and analysis platform. **2012**. *J Cheminform*, 4, <https://doi.org/10.1186/1758-2946-4-17>
38. Pettersen, E. F.; Goddard, T. D.; Huang, C. C.; Couch, G. S.; Greenblatt, D. M.; Meng, E. C.; Ferrin, T. E. UCSF Chimera—A visualization system for exploratory research and analysis. **2004**. *J Comput Chem*, 25, 1605–1612. <https://doi.org/10.1002/jcc.20084>

39. Eberhardt, J.; Santos-Martins, D.; Tillack, A. F.; Forli, S. AutoDock Vina 1.2.0: New docking methods, expanded force field, and python bindings. **2021**. J Chem Inf Model, 61, 3891–3898. <https://doi.org/10.1021/acs.jcim.1c00203>
40. Yan, Y.; Tao, H.; He, J.; Huang, S.-Y. The HDock server for integrated protein-protein docking. **2020**. Nat Protoc, 15, 1829–1852. <https://doi.org/10.1038/s41596-020-0312-x>
41. Schmitt, M. E.; Brown, T. A.; Trumpower, B. L. A rapid and simple method for preparation of RNA from *Saccharomyces cerevisiae*. **1990**. Nucleic Acids Res, 18, 3091–3092. <https://doi.org/10.1093/nar/18.10.3091>
42. Livak, K. J.; Schmittgen, T. D. Analysis of relative gene expression data using real-time quantitative PCR and the 2- $\Delta\Delta$ CT method. **2001**. Methods, 25, 402–408. <https://doi.org/10.1006/meth.2001.1262>
43. Carolus, H.; Pierson, S.; Muñoz, J. F.; Subotić, A.; Cruz, R. B.; Cuomo, C. A.; Van Dijk, P. Genome-wide analysis of experimentally evolved *Candida auris* reveals multiple novel mechanisms of multidrug resistance. **2021**. mBio, 12, e03333-20. <https://doi.org/10.1128/mbio.03333-20>
44. Hager, C. L.; Larkin, E. L.; Long, L.; Zohra Abidi, F.; Shaw, K. J.; Ghannoum, M. A. In vitro and in vivo evaluation of the antifungal activity of APX001A/APX001 against *Candida auris*. **2018**. Antimicrob Agents Chemother, 62. <https://doi.org/10.1128/AAC.02319-17>
45. Bras, G.; Satala, D.; Juszczak, M.; Kulig, K.; Wronowska, E.; Bednarek, A.; Karkowska-Kuleta, J. Secreted aspartic proteinases: Key factors in *Candida* infections and host-pathogen interactions. **2024**. Int J Mol Sci, 25, 4775. <https://doi.org/10.3390/ijms25094775>
46. Gagnon-Arsenault, I.; Parisé, L.; Tremblay, J.; Bourbonnais, Y. Activation mechanism, functional role and shedding of glycosylphosphatidylinositol-anchored Yps1p at the *Saccharomyces cerevisiae* cell surface. **2008**. Mol Microbiol, 69, 982–993. <https://doi.org/10.1111/j.1365-2958.2008.06339.x>
47. Rasheed, M.; Battu, A.; Kaur, R. Aspartyl proteases in *Candida glabrata* are required for suppression of the host innate immune response. **2018**. J Biol Chem, 293, 6410–6433. <https://doi.org/10.1074/jbc.M117.813741>
48. Olsen, V.; Cawley, N. X.; Brandt, J.; Egel-Mitani, M.; Loh, Y. P. Identification and characterization of *Saccharomyces cerevisiae* yapsin 3, a new member of the yapsin family of aspartic proteases encoded by the YPS3 gene. **1999**. Biochem J, 339, 407–411. <https://doi.org/10.1042/bj3390407>
49. Dubé, A. K.; Bélanger, M.; Gagnon-Arsenault, I.; Bourbonnais, Y. N-terminal entrance loop of yeast Yps1 and O-glycosylation of substrates are determinant factors controlling the shedding activity of this GPI-anchored endopeptidase. **2015**. BMC Microbiol, 15, 1–14. <https://doi.org/10.1186/s12866-015-0380-1>
50. Vadaie, N.; Dionne, H.; Akajagbor, D. S.; Nickerson, S. R.; Krysan, D. J.; Cullen, P. J. Cleavage of the signaling mucin Msb2 by the aspartyl protease Yps1 is required for MAPK activation in yeast. **2008**. J Cell Biol, 181, 1073–1081. <https://doi.org/10.1083/jcb.200704079>
51. Miller, K. A.; DiDone, L.; Krysan, D. J. Extracellular secretion of overexpressed glycosylphosphatidylinositol-linked cell wall protein Utr2/Crh2p as a novel protein quality control mechanism in *Saccharomyces cerevisiae*. **2010**. Eukaryot Cell, 9, 1669–1679. <https://doi.org/10.1128/EC.00191-10>
52. Chatterjee, S.; Alampalli, S. V.; Nageshan, R. K.; Chettiar, S. T.; Joshi, S.; Tatu, U. S. Draft genome of a commonly misdiagnosed multidrug resistant pathogen *Candida auris*. **2015**. BMC Genomics, 16, 686. <https://doi.org/10.1186/s12864-015-1863-z>
53. Zhang, Y. Progress and challenges in protein structure prediction. **2008**. Curr Opin Struct Biol, 18, 342–348. <https://doi.org/10.1016/j.sbi.2008.02.004>
54. Shimizu, N.; Katagiri, T.; Matsumoto, A.; Matsuda, Y.; Arai, H.; Sasaki, N.; Abe, K.; Katase, T.; Ishida, H.; Kusumoto, K. I.; Takeuchi, M.; Yamagata, Y. Oryzapsins, the orthologs of yeast yapsin in *Aspergillus oryzae*, affect ergosterol synthesis. **2021**. Appl Microbiol Biotechnol, 105, 8481–8494. <https://doi.org/10.1007/s00253-021-11639-7>
55. Silva, R. D. S.; Segura, W. D.; Oliveira, R. S.; Xander, P.; Batista, W. L. Characterization of aspartic proteases from *Paracoccidioides brasiliensis* and their role in fungal thermo-dimorphism. **2023**. J Fungi, 9, 375. <https://doi.org/10.3390/jof9030375>
56. Clark-Flores, D.; Vidal-Montiel, A.; Mondragón-Flores, R.; Valentín-Gómez, E.; Hernández-Rodríguez, C.; Juárez-Montiel, M.; Villa-Tanaca, L. Vacuolar proteases of *Candida auris* from clades III and IV and their relationship with autophagy. **2025**. J Fungi, 11, 388. <https://doi.org/10.3390/jof11050388>

57. Day, A. M.; McNiff, M. M.; da Silva Dantas, A.; Gow, N. A.; Quinn, J. Hog1 regulates stress tolerance and virulence in the emerging fungal pathogen *Candida auris*. **2018**. mSphere, 3. <https://doi.org/10.1128/mSphere.00506-18>
58. Gibbs, E.; Hsu, J.; Barth, K.; Goss, J. W. Characterization of the nanomechanical properties of the fission yeast (*Schizosaccharomyces pombe*) cell surface by atomic force microscopy. **2021**. Yeast, 38, 480–492. <https://doi.org/10.1002/yea.3564>
59. Bairwa, G.; Rasheed, M.; Taigwal, R.; Sahoo, R.; Kaur, R. GPI (glycosylphosphatidylinositol)-linked aspartyl proteases regulate vacuole homeostasis in *Candida glabrata*. **2014**. Biochem J, 458, 323–334. <https://doi.org/10.1042/BJ20130757>
60. Shivarathri, R.; Chauhan, M.; Datta, A.; Das, D.; Karuli, A.; Aptekmann, A.; Chauhan, N. The *Candida auris* Hog1 MAP kinase is essential for the colonization of murine skin and intradermal persistence. **2024**. mBio, 15, e02748-24. <https://doi.org/10.1128/mbio.02748-24>
61. Banda-Flores, I. A.; Torres-Tirado, D.; Mora-Montes, H. M.; Pérez-Flores, G.; Pérez-García, L. A. Resilience in resistance: The role of cell wall integrity in multidrug-resistant *Candida*. **2025**. J Fungi, 11, 271. <https://doi.org/10.3390/jof11040271>
62. Cortés-Acosta, E.; Ibarra, J. A.; Ramírez-Saad, H.; Vargas-Mendoza, C. F.; Villa-Tanaca, L.; Hernández-Rodríguez, C. Polymorphism in the regulatory regions of genes *CgYPS1* and *CgYPS7* encoding yapsins in *Candida glabrata* is associated with changes in expression levels. **2017**. FEMS Yeast Res, 17, fox077. <https://doi.org/10.1093/femsyr/fox077>
63. Mercurio, K.; Singh, D.; Walden, E.; Baetz, K. Global analysis of *Saccharomyces cerevisiae* growth in mucin. **2021**. G3, 11, jkab294. <https://doi.org/10.1093/g3journal/jkab294>
64. Jenull, S.; Tscherner, M.; Kashko, N.; Shivarathri, R.; Stoiber, A.; Chauhan, M.; Petryshyn, A.; Chauhan, N.; Kuchler, K. Transcriptome signatures predict phenotypic variations of *Candida auris*. **2021**. Front Cell Infect Microbiol, 11, 662563. <https://doi.org/10.3389/fcimb.2021.662563>

Disclaimer/Publisher's Note: The statements, opinions and data contained in all publications are solely those of the individual author(s) and contributor(s) and not of MDPI and/or the editor(s). MDPI and/or the editor(s) disclaim responsibility for any injury to people or property resulting from any ideas, methods, instructions or products referred to in the content.